of the crystal was periodically changed by a heat leak from 1.5°K to 7°K. A small, reversible, and reproducible anisotropy of about $\frac{1}{2}\%$ was observed, several times larger than background noise. The sign of the anisotropy reversed after the crystal was rotated through 90°, as expected; the sign did not change on rotation of 180°. From this experiment we can conclude definitely that $I(\mathrm{Np}^{239})>\frac{1}{2}$, since a γ-ray anisotropy is not possible for nuclei with $I=\frac{1}{2}$. This result is consistent with that of Hubbs and Marrus,[5] who find $I(\mathrm{Np}^{239})=\frac{5}{2}$ by radioactive atomic beam methods.

[5] J. C. Hubbs and R. Marrus, Phys. Rev. **110**, 287 (1958).

PHYSICAL REVIEW VOLUME 112, NUMBER 2 OCTOBER 15, 1958

Photoneutron Yields in the Rare-Earth Region*

E. G. Fuller, B. Petree, and M. S. Weiss†
National Bureau of Standards, Washington, D. C.

(Received June 16, 1958)

The total photoneutron yield curves for Sn, I, La, Ce, Sm, Tb, Ho, Er, Yb, Ta, Au, and Pb have been measured for x-ray energies from 7 to 40 Mev with about one percent statistical uncertainty. The Penfold-Leiss matrix was used to convert these yield curves to *integrated* neutron yield cross sections directly without smoothing the original activation curves. The cross sections derived from the integral curves were corrected for multiple neutron emission above the $(\gamma,2n)$ threshold using the statistical model. The widths found for the giant resonances for the closed-shell nuclei decreased from 5 Mev to 3.8 Mev in going from Sn to Pb. The widths for the elements having large nuclear deformations for most of their isotopes were considerably broader. These widths decreased slowly from 8.6 Mev for Sm to 6 Mev for Ta. These widths are consistent with the broadening of the giant resonance to be expected on the Danos model if values of the intrinsic quadrupole moment are taken from Coulomb excitation data. The neutron yield cross sections corrected for multiple neutron emission were integrated to 22 Mev. Using these integrals and defining f by $\int\sigma dE=0.06(NZ/A)f$, these data gave an average value of $f=1.34\pm0.21$.

INTRODUCTION

It has recently been suggested by both Okamoto[1] and Danos[2] independently that on a classical hydrodynamic model of the nucleus one might expect the giant resonance for a deformed unoriented nucleus to be split into two resonances. These two resonances would be associated with the major and minor axes of the nucleus. In the case of a nucleus with positive intrinsic quadrupole moment the "giant resonance" would be made up of a low-energy resonance shifted to an energy slightly lower than that expected for a spherical nucleus of the same mass number and a high-energy resonance shifted to a slightly higher energy. Danos[2] has pointed out that the area under the low-energy resonance would be one-half that under the higher energy resonance.

In a "poor resolution" measurement of the giant resonance the splitting resulting from the ground-state deformation would not be observable. The effect of the deformation might, however, show up as a statistically significant broadening in the giant resonance compared to that obtained for a nearby spherical nucleus. Consistent with this picture is the observation of the Pennsylvania group[3] that the giant resonances for closed-shell nuclei are narrower than those in general observed for other nuclei. It was the object of the present work to see if the large intrinsic quadrupole moments of the rare earth nuclei were reflected in the total width of the giant resonance for these nuclei. The total neutron yield curve was measured for a series of twelve nuclei ranging from tin through the rare earths to lead. Measurements were made from the (γ,n) threshold in each element up to about 40 Mev. The samples were all of normal isotopic abundance. The preliminary results of this work have been reported previously.[4]

EXPERIMENTAL APPARATUS AND PROCEDURES

The method used in this study was similar to that which has previously been used in studies of the total neutron yields from various elements.[3,5] The experiment consisted of measuring the number of neutrons emitted from a series of samples as a function of the peak betatron operating energy. The experimental arrangement is shown in Fig. 1. The neutron detector is of conventional design[5] containing eleven BF_3 counters connected in parallel. The amplified pulses from the

* This work supported by the U. S. Atomic Energy Commission.
† Presently on educational leave at the Massachusetts Institute of Technology, Cambridge, Massachusetts.
[1] K. Okamoto, Progr. Theoret. Phys. Japan **15**, 75 (1956).
[2] M. Danos, Bull. Am. Phys. Soc. Ser. II, **1**, 199 (1956); Nuclear Phys. **5**, 23 (1958).
[3] R. Nathans and J. Halpern, Phys. Rev. **73**, 437 (1954); R. Nathans and P. F. Yergin, Phys. Rev. **98**, 1296 (1955).
[4] Fuller, Petree, and Weiss, Chicago Photonuclear Conference, November 1956 (unpublished report); Petree, Weiss, and Fuller, Bull. Am. Phys. Soc. Ser. II, **2**, 16 (1957).
[5] Halpern, Mann, and Nathans, Rev. Sci. Instr. **23**, 678 (1952).

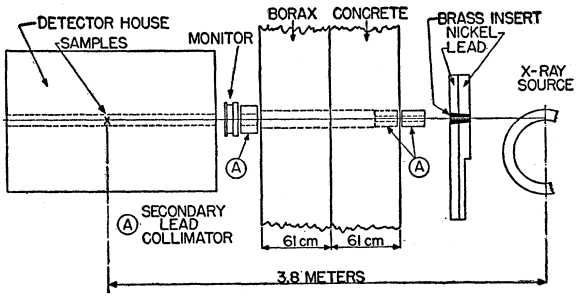

FIG. 1. Experimental arrangement. X-ray beam is collimated by brass insert in nickel and lead shielding wall.

counters after passing through an integral discriminator were gated so that only those pulses occurring within a 400-μsec gate were counted. The sensitivity of the detector was checked as follows:

Its absolute sensitivity was determined daily by placing a calibrated Ra-Be (α,n) source inside the detector and observing the counting rate.[6] The uniformity of the response of the detector to fast neutrons was shown by the fact that the ratio of the neutron yield from a carbon sample placed inside the detector to the yield of $C^{12}(\gamma,n)C^{11}$ activity induced in a sample exposed to the same beam was constant as the bremsstrahlung energy was varied by about 4 Mev. In addition, the ratio of the calculated neutron yield to the measured yield from the deuterium in a heavy water sample was constant to within 4% as the bremsstrahlung energy was varied from 6 to 19 Mev.

The 400-μsec gate, used when counting the photoneutrons from samples placed inside the detector, was set to open about 20 μsec after the x-ray yield pulse. Studies made of the distribution of these counts with respect to time after the x-ray burst indicated that 82% of all the counts occurred during the period that the gate was open. Combining this with the efficiency of 6.3% found for the continuous Ra-Be $(\alpha$-$n)$ neutron source gave an over-all neutron detection efficiency of 5.2%.

The energy flux in the bremsstrahlung beam produced by the betatron was determined from the charge collected from the thin aluminum-walled transmission ionization-chamber monitor shown in Fig. 1. The response of this chamber in terms of the energy flux incident on its front face was determined by comparison with a chamber which had previously been calibrated over the energy range from 8 to 40 Mev by one of us (E.G.F.) using the scintillation spectrometer method.[7]

The energy scale of the betatron was determined by observing the threshold for scattering by the 15.11-Mev level in C^{12}, and by the (γ,n) thresholds in H^2 (2.2 Mev), Pb^{207} (6.75 Mev), Au^{197} (8.0 Mev), Cu^{65} (9.85 Mev), and Al^{27} (12.8 Mev). These thresholds fell on a straight line when plotted against the betatron's energy control setting. A linear extrapolation of this curve was used to give the energies above 15 Mev. This extrapolation has been shown to be valid to better than 5% by the endpoint determinations made in the elastic scattering experiment.[8]

TABLE I. Target properties and results.

Element	Form used	Weight grams	$\sigma^0(\gamma,n)$[a] barns	$\frac{S\sigma dE}{NZ/A}$[b] Mev-b	"I"[a] Mev
Sn	Sn	4.81	0.30	0.064	5.0
I	I	8.55	0.36	0.085	6.0
La	La	10.43	0.34	0.063	5.2
Ce	Ce	4.99	0.45	0.080	4.5
Sm	Sm_2O_2	2.90	0.26	0.073	8.6
Tb	Tb_4O_7	3.04	0.39	0.087	8.7
Ho	Ho_2O_3	1.87	0.41	0.079	7.5
Er	Er_2O_3	5.41	0.50	0.100	8.5
Yb	Yb_2O_3	5.57	0.50	0.090	7.0
Ta	Ta	8.41	0.49	0.077	6.0
Au	Au	3.16	0.68	0.085	4.2
Pb	Pb	8.05	0.75	0.081	3.8

[a] $\sigma^0(\gamma,n)$ is the maximum value and "I" the full width at $\sigma^0(\gamma,n)/2$ of the neutron production cross section corrected for multiple neutron emission. Data were not fitted with resonance lines to determine these values.
[b] Integrated neutron production cross sections corrected for multiple neutrons above $(\gamma,2n)$ threshold.

Table I gives the properties of the various elements from which the neutron yield was measured. The rare-earth oxides were all exposed in thin polyethylene cylinders of about 1 square centimeter in cross section. The samples were exposed in the center of the neutron detector with their axes parallel to the x-ray beam running through the detector. All samples except the lead were smaller in diameter than the beam. The electronic absorption in the samples was usually about 10% but was as high as 25% in the case of lanthanum.

The total neutron yield from each of the samples listed in Table I was measured as a function of bremsstrahlung energy from the (γ,n) threshold up to about 40 Mev. From threshold to about 19-Mev data were taken approximately every 600 kev. Above 19-Mev data were taken approximately every 1.2 Mev. At each point the neutron yield was measured with a statistical uncertainty $(1/\sqrt{n})$ of about 1% except in the energy region near threshold.

The activation curve for each sample was measured by taking data at a series of either continuously increasing or decreasing energy points. This method of taking data had the advantage that the effects of any small drifts in the betatron's energy calibration on the shape of the cross section derived from the activation curve were minimized. Any such shifts were shown to be less than 100 kev at 18 Mev by periodically checking the neutron yield from a copper sample at this energy.

[6] The absolute sensitivity for detecting 30-kev neutrons was also determined by placing a calibrated Sb-Be photoneutron source within the detector. As might be expected [B. Rossi and H. H. Staub, *Ionization Chambers and Counters* (McGraw-Hill Book Company, Inc., New York, 1949), p. 192], the sensitivity for these neutrons was approximately 75% of that found for the Ra-Be (α,n) source.

[7] Koch, Leiss, and Pruitt, Bull. Am. Phys. Soc. Ser. II, **1**, 199 (1956).

[8] E. G. Fuller and E. Hayward, Phys. Rev. **101**, 692 (1956).

For bremsstrahlung energies greater than 20 Mev it was necessary to interrupt the measurements every forty minutes to cool the betatron. After a cooling period, the previous two or three points on the activation curve were always repeated before proceeding to new energies. Measurements were continued only when the yields measured after a cooling break agreed with those taken just before the break. At times it was necessary to run the betatron for five to ten minutes before reproducible results were obtained.

The background was determined by measuring the activation curve for the empty sample holder. This background amounted to less than 3% of the neutron yield from any of the samples. In order to correct for the oxygen contribution to the neutron yield from the rare earth oxides, the neutron yield from a water sample was measured up to 40 Mev. This correction amounted to a maximum of 5%. At the higher energies and from the larger samples it was necessary to cut down the yield from the betatron in order to keep counting losses to a minimum. The correction for this effect was determined by measuring the neutron yield at a given energy as a function of the time taken to collect a given charge from the transmission ionization chamber. This correction was as high as 5% in a few cases, but usually was less than 3%.

ANALYSIS OF THE DATA

The fact that large fluctuations are obtained in a cross section calculated directly from the experimental data of a yield curve measured with 1% statistical accuracy has led to the usual procedure of drawing a smooth curve through the measured yield points.[9] These curves are sometimes smoothed as far as the second differences. While this smoothing has the desired effect of reducing fluctuations in the cross section it may smooth out real structure. In addition, since small changes in the way that a smooth yield curve is drawn through the experimental points can produce large changes in the cross section, the method is highly subjective. The best way to overcome these difficulties is to measure yield curves with sufficient accuracy as to make possible the calculation of a statistically significant cross section from the actual experimental data without smoothing. To do this would require the measurement of the yield curve with a statistical accuracy of at least one order of magnitude better than the measurements made in this experiment.

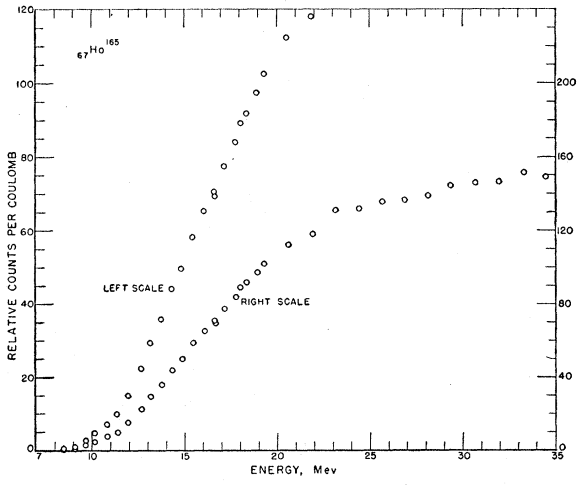

FIG. 2. Measured neutron yield curve for holmium. The points represent the relative number of neutrons per coulomb collected from transmission ionization chamber. Corrections have been made for background and the oxygen content of the sample.

[9] L. Katz and A. G. W. Cameron, Can. J. Phys. **29**, 518 (1951).

Since the data taken in this experiment were not of sufficient statistical accuracy to allow the cross section to be calculated directly from the experimental data, the method of analysis used was one based in part on a suggestion by Cook.[10] The method consisted of using the inverse bremsstrahlung matrix of Penfold and Leiss[11] to calculate the *integrated* neutron cross section as a function of the upper energy limit of the integral. The experimental data points were used without any smoothing to calculate this running integral. A smooth curve was then drawn through these points. First differences of these curves were then taken to give the cross section histograms. Recent measurements, with similar geometry, of the shape of the bremsstrahlung spectrum from the betatron used in this experiment show that the use of the Penfold-Leiss tables to analyze these data is well justified.[12]

The advantages of this type of analysis are numerous. Both the integral cross section, $I(E_0)$, calculated in this way and the cross section, $\sigma(E_i)$, obtained by taking the first difference of $I(E_0)$ are well defined in terms of the true cross section, $\sigma(E)$. Leiss and Penfold[11,13] have shown that

$$I(E_0)=\sum\sigma(E_i)\Delta E=\int_0^{E_0}\sigma(E)T'(E,E_0)dE,$$

where $T'(E,E_0)$ is a weighting function defined in terms of the inverse matrix. This function has been shown to a good approximation to have the value one up to $(E_0-\Delta E)$ and to then fall off with the shape of a bremsstrahlung spectrum having a maximum energy E_0. Similarly these authors have shown that $\sigma(E_i)$ derived from $I(E_0)$ is very closely given by the average over ΔE of the true cross section weighed with a function having the shape of a bremsstrahlung spectrum with a maximum energy $(E_i+\frac{1}{2}\Delta E)$.

A further advantage of this type of analysis is that the statistical errors for $I(E_0)$ can be obtained directly

[10] B. C. Cook, Phys. Rev. **106**, 300 (1957).
[11] A. S. Penfold and J. E. Leiss, Phys. Rev. **95**, 637(A) (1954).
[12] Fuller, Hayward, and Koch, Phys. Rev. **109**, 630 (1958).
[13] J. E. Leiss (private communication). See also, A. S. Penfold and J. E. Leiss, *Analysis of Photo Cross Sections* (Physics Research Laboratory, University of Illinois, Champaign, Illinois, 1958).

by propagating the errors of the individual points of the activation curve through the inverse matrix. It can be shown for a typical activation curve that the errors in $I(E_0)$ while being considerably larger than those associated with the original points on the activation curve are about 2.5 times less than those that would be obtained by summing the errors on the individual cross section points in the usual way. $I(E_0)$ is then fairly well determined by a 1% activation curve. For such a typical curve the statistical errors range from 4% where the cross section is rising, to 6% on the high-energy side of the giant resonance, to 11% at 38 Mev. It should be pointed out that by not smoothing the experimental data until the curve $I(E_0)$ has been obtained it is possible to see directly the effects of smoothing on the final cross section $\sigma(E_i)$.

The data for this experiment were unfortunately taken at fixed settings of the betatron energy control

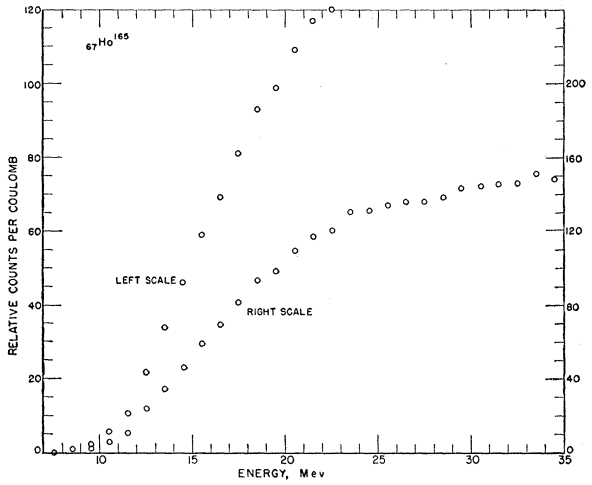

FIG. 3. "Shifted" neutron yield curve for holmium. For description see text.

rather than at the definite energies required for use with the Penfold-Leiss matrix. This procedure of taking data required that the data be shifted so that they could be used with the inverse matrix available. This shift was accomplished as follows: The data were plotted after making corrections for target-out background and the oxygen content of the sample. As an example, Fig. 2 gives a plot of the measured yield curve from holmium. A smooth curve was drawn by eye through these points. The slope of this curve was used to shift the experimentally observed points to the energies required for use with the Leiss-Penfold matrix. These data are plotted in Fig. 3 for holmium. Each point on this curve was obtained by shifting the nearest, or in some cases, the two nearest experimental points to the energy required for the inverse matrix. These points contain all of the experimental fluctuations in the original data points. The Leiss-Penfold matrix was

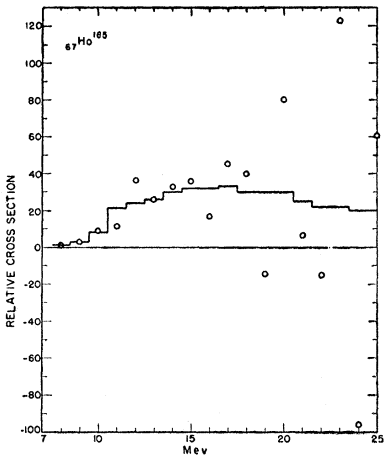

FIG. 4. Neutron yield cross section. The points represent the cross section obtained by applying the Leiss-Penfold matrix directly to the points of Fig. 3. The histogram is the result of taking the first differences of the smoothed integral cross section curve given in Fig. 5(b).

then applied to these data to obtain the cross section which was then summed to give the integral cross-section curve plotted in Fig. 5(b). In Fig. 4 the raw cross section obtained from the unsmoothed data points is compared with the histogram obtained from the smoothed integral cross-section curve drawn through the points in Fig. 5(b). The fluctuations in these points are completely consistent with the statistical errors in the original data.

RESULTS AND DISCUSSION

The integral cross-section curves for six of the twelve elements studied are given in Figs. 5(a) and 5(b). The solid histograms in these figures are the total neutron yield cross sections obtained by taking first differences of the smooth integral cross section curve. These curves have all been normalized to give approximately the same total neutron yield at 40 Mev. Since these cross sections represent the total neutron yield rather than the photon absorption cross section, the giant resonance indicated by them is broadened by the effects of multiple neutron emission above the $(\gamma,2n)$ threshold. The dashed histograms represent an attempt to correct for multiple neutron emission. This correction was made using the expression for neutron multiplicity based on the statistical model as given by Blatt and Weisskopf.[14] This expression has been shown to give an approximately correct description of the $(\gamma,2n)$ process in the case of tantalum.[15] The nuclear temperature used in these calculations ranged from 1.4 Mev for tin to 1.25 Mev for lead. For nuclei up to samarium the $(\gamma,2n)$

[14] J. M. Blatt and V. F. Weisskopf, *Theoretical Nuclear Physics* (John Wiley and Sons, Inc., New York, 1952), p. 379.

[15] E. A. Whalin and A. O. Hanson, Phys. Rev. **89**, 324 (1953); Carver, Edge, and Lokan, Proc. Roy. Soc. (London) **A70**, 415 (1957).

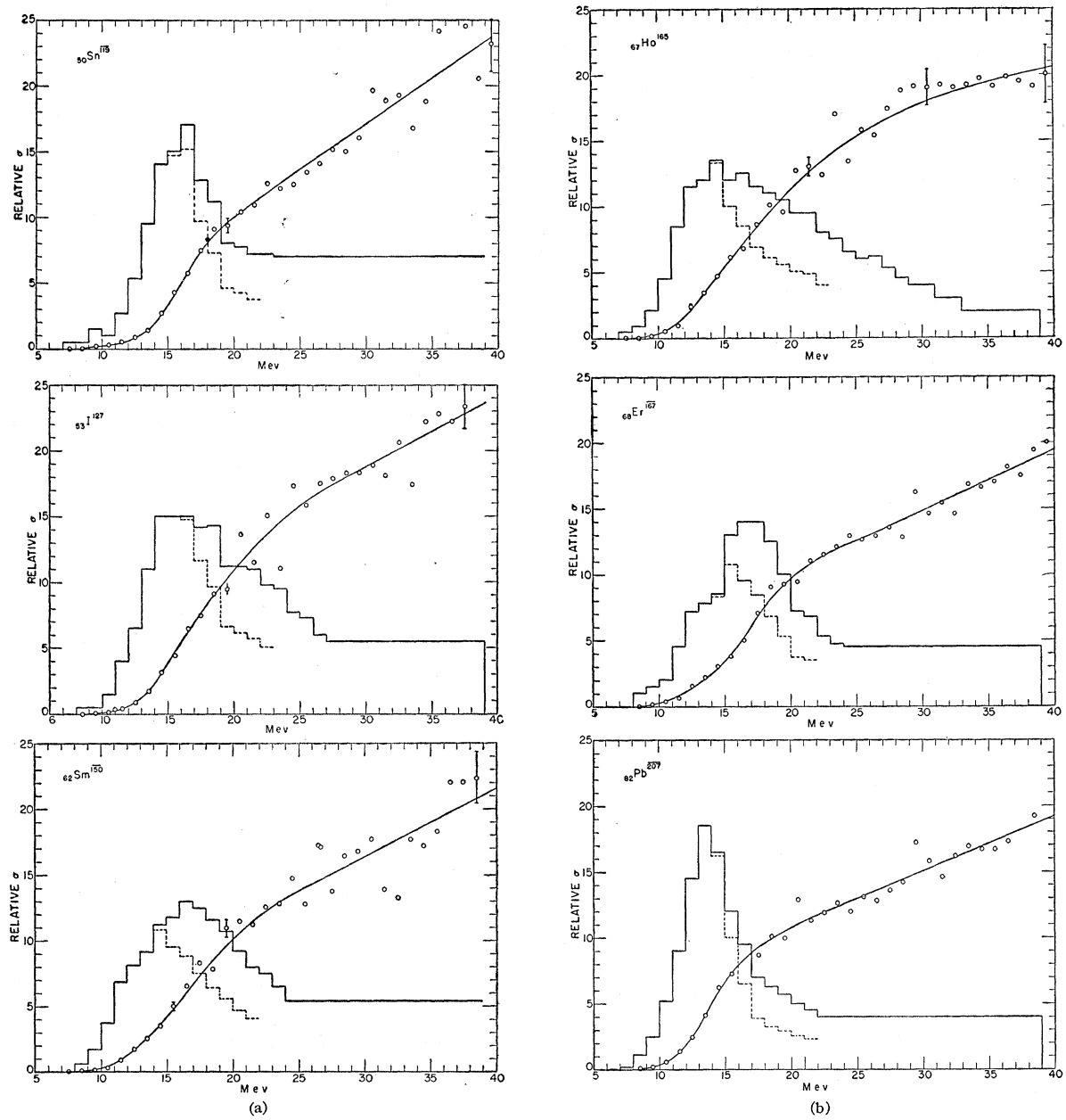

FIG. 5. Relative photoneutron production cross sections for tin, iodine, samarium, holmium, erbium, and lead. The points and smooth curves represent the integral neutron-production cross section defined by $\int_0^E \sigma_{Tn}(E)dE$, where $\sigma_{Tn}(E)=\sigma(\gamma,n)+2\sigma(\gamma,2n)+\sigma(\gamma,pn)+3\sigma(\gamma,3n)+\ldots$. The scales are normalized to give approximately the same total neutron yield at 40 Mev. The errors indicated were obtained by propagating the statistical uncertainties, $(\sqrt{n})$, in the original activation curve data through the integral cross section matrix. Solid histograms represent first differences of integral cross section curves. Dashed histograms show result of correcting for neutron multiplicity above the $(\gamma,2n)$ threshold.

thresholds were taken from the binding energies as given by Johnson and Nier and in the compilation by Wapstra.[16] For the other nuclei the binding energies were calculated from Levy's semiempirical mass formula.[17] No attempt was made to correct for multiple neutron emission above the $(\gamma,3n)$ threshold. The dashed histograms indicate that the use of a neutron-multiplicity correction based on a more detailed calculation and extending to higher energies would have the effect of greatly decreasing the high-energy tail shown by the total neutron-yield cross section. It is obvious from the figures that correcting the total neutron-yield cross section for two-neutron emission both removes

[16] W. H. Johnson and A. O. Nier, Phys. Rev. **105**, 1014 (1957); A. H. Wapstra, Physica **21**, 367 (1955).
[17] H. B. Levy, Phys. Rev. **106**, 1265 (1957).

TABLE II. Energies of resonances in deformed nuclei.[a]

Nucleus	E_m Mev	Q_0 barns	Method	E_a Mev	E_b Mev	$E_{1/2}^-$ Mev	$E_{1/2}^+$ Mev
$_{65}Tb^{159}$	14.7	6.9[b]	CE	11.9	16.2	10.8	19.5
$_{67}Ho^{165}$	14.5	7.8[b]	CE	11.5	16.0	11.0	18.5
$_{68}Er^{167}$	14.5	21[b]	SC	8.5	17.5	11.5	20.0
$_{68}Er^{164}$	14.5	7.8[b]	CE	11.6	15.9	11.5	20.0
$_{73}Ta^{181}$	14.1	12.6[c]	SC	10.5	15.9	11.3	17.3
$_{73}Ta^{181}$	14.1	6.8[b]	CE	11.9	15.2	11.3	17.3
$_{79}Au^{197}$	13.6	3.75[c]	SC	12.5	14.1	11.8	16.2

[a] CE—Coulomb excitation; SC—spectroscopic; $E_{1/2}^-$, $E_{1/2}^+$—energies at which giant resonance drops to half its maximum value.
[b] Adler, Bohr, Huus, Mottelson, and Winther, Revs. Modern Phys. **28**, 432 (1956).
[c] M. L. Pool and D. N. Kundu, *Chart of Atomic Nuclei* (Longs College Book Company, Columbus, 1955).

some of the fluctuations in the shape of the giant resonance from one nucleus to another and makes the cross sections more symmetrical about some mean energy.

The absolute neutron-yield cross sections as well as the parameters of the giant resonance for the nuclei studied in this experiment are summarized in Table I and Fig. 6. The widths and the energies of the center of the giant resonance for these nuclei are determined to within 0.5 Mev by these data. The values quoted for the integrated (γ,n) cross section up to 22 Mev are probably good to about 20%. Of this uncertainty about 10% results from counting statistics. The remainder is the result of uncertainties in the size of the beam through the neutron detector ($\pm 15\%$), in the correction for multiple neutrons ($\pm 5\%$), and in the monitor calibration ($\pm 3\%$). Similarly the peak cross sections are good to about 25%.

The integral cross sections corrected for neutron multiplicity can be compared with the result given by the dipole sum rule.[18] This can be written as

$$\int \sigma dE = 0.06 \frac{NZ}{A} f,$$

where f is the factor by which the sum for ordinary forces is enhanced as a result of the presence of exchange forces. The cross sections corrected for neutron multiplicity as given in Fig. 5 have been summed to give the total integrated cross section up to 22 Mev. These data, divided by NZ/A, are given in Table I. Within the errors of the individual points each one is consistent with a single value of f for all of these nuclei. Averaging the individual values gives $f=1.34\pm 0.21$. This value of f should be increased by a maximum of about 15% to take into account the fact that the integral of the cross sections given in Fig. 5 does not represent the complete integral of the absorption cross section. This estimate is the result of fitting several of the curves for closed-shell nuclei with Lorentz lines and integrating these cross sections over all energies.

The mean energy of the giant resonance as plotted in Fig. 6 is consistent with an $A^{-\frac{1}{3}}$ dependence although the $A^{-1/6}$ dependence cannot be completely ruled out as

[18] J. S. Levinger and H. A. Bethe, Phys. Rev. **78**, 115 (1950).

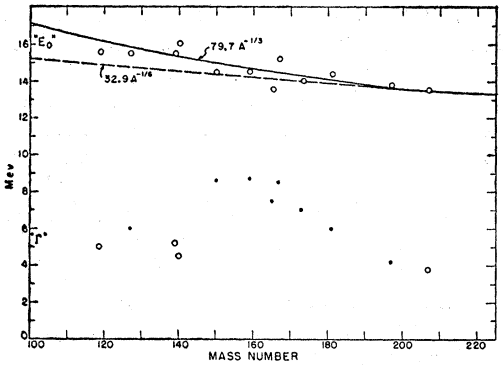

FIG. 6. Mean energy and width of giant resonances. "E_0" and "Γ" are the mean energy for photon absorption and the full width at half maximum of the giant resonance obtained from dashed histograms as in Fig. 5. No attempt was made to fit data with resonance curves to obtain these parameters.

inconsistent with these data. The width of the giant resonance as given in Table I and Fig. 6 broadens rapidly at samarium, the first element studied having isotopes in the region of large nuclear deformations. The widths then slowly decrease as the closed-shell region at lead is approached. These data are not sufficiently accurate to be able to establish the existence of a double peak for the deformed nuclei as predicted by Danos and Okamoto. The integral cross section curves for these nuclei, however, are not inconsistent with such a cross section shape. Further work has been carried out in this laboratory to establish this feature of the giant resonance for some of these nuclei.[19]

For a deformed nucleus, the width of the giant resonance measured with poor resolution results from the intrinsic widths associated with the individual resonances and the separation of these resonances. Qualitative estimates can be made for the widths to be expected based on measured quadrupole moments, but good-resolution experiments are required before any quantitative results can be obtained. These estimates can be made in the following way. The mean energy of the giant resonance for a deformed nucleus is given approximately by

$$E_m = (E_a + 2E_b)/3,$$

where a and b refer to the major and minor axes of the nucleus. Danos[2] has shown that the relation between E_a, E_b, and these axes is given by

$$E_b/E_a = 0.911X + 0.089,$$

where $X=a/b$, the ratio of the major to minor axis. In terms of a and b the intrinsic quadrupole moment is given by

$$Q_0 = \tfrac{2}{5}Z(a^2-b^2) = \tfrac{2}{5}ZR_0^2A^{\frac{2}{3}}(X^2-1)/X^{\frac{2}{3}}$$

where R_0 is the constant in the expression for the nuclear radius $R=R_0A^{\frac{1}{3}}$.

[19] See E. G. Fuller and M. S. Weiss, Phys. Rev. **112**, 560 (1958), following paper.

Values of the intrinsic quadrupole moment can be obtained from spectroscopic and from Coulomb excitation data. Using the expression $E_m=79.7A^{-\frac{1}{3}}$ to give the mean energy for the giant resonance and measured values of the quadrupole moments, the energies E_a and E_b can be calculated from the above expressions. The results of several such calculations are given in Table II. If the intrinsic widths associated with the two axes are assumed to be the same as that for an undeformed nucleus, i.e., approximately 4 Mev, the half-maximum points would be expected to occur about 2 Mev below E_a and 2 Mev above E_b. The last two columns of Table II give the half-maximum points obtained from Fig. 5. In comparing these energies it should be pointed out that the value of $E_{\frac{1}{2}}^+$ will depend much more critically on the correction made for neutron multiplicity than will the value of $E_{\frac{1}{2}}^-$. The values of E_a and E_b calculated from the Coulomb-excitation-derived quadrupole moments are in reasonable agreement with the half-maximum energies found in this experiment. Since the large quadrupole moments obtained from the spectroscopic measurements give values of E_a less than the half-maximum energy $E_{\frac{1}{2}}^-$, these moments are in disagreement with the widths obtained for these giant resonances.

ACKNOWLEDGMENTS

The authors wish to thank M. Danos and J. E. Leiss for many fruitful discussions.

PHYSICAL REVIEW VOLUME 112, NUMBER 2 OCTOBER 15, 1958

Splitting of the Giant Resonance for Deformed Nuclei*

E. G. FULLER AND M. S. WEISS†
National Bureau of Standards, Washington, D. C.
(Received June 16, 1958)

Photoneutron yield measurements have been made for terbium, tantalum, and gold with good energy resolution from threshold up to 25 Mev. Neutron-production cross sections were obtained directly from the experimental points without smoothing the raw data. Corrections were made for the multiple production of neutrons above the $(\gamma,2n)$ thresholds. The giant resonances for terbium and tantalum were found to be split into two resonances as predicted by Okamoto and Danos. The giant resonances for all three nuclei were fitted by the superposition of two Lorentz shape resonance lines. The intrinsic quadrupole moments determined from these fits to the experimental data were: terbium, $+5.6\pm0.6$ barns; tantalum, $+5.7\pm0.3$ barns; and gold, $+1.6\pm0.6$ barns.

1. INTRODUCTION

THE giant resonances of closed-shell nuclei have been observed to be appreciably narrower than those of nuclei situated between closed shells.[1] Previous work[2] in this laboratory indicated that the giant resonances of the rare-earth nuclei were larger than any previously observed. While not established by that experiment, the data obtained for terbium, holmium, erbium, ytterbium, and tantalum were consistent with the giant resonance for these nuclei being split into two peaks. These results were all in accord with the predictions of Okamoto[3] and Danos[4] that the giant resonance for a deformed nucleus should be split into two resonances. The extension of the hydrodynamical model for the nuclear photoeffect[5] made by Okamoto and Danos leads to a giant resonance energy being associated with each of the axes of a deformed nucleus.[3-4]

It was the object of the present work to examine with good energy resolution the details of the shape of the giant resonance for two highly deformed nuclei and of one having a considerably smaller deformation to see if the details of the resonance shapes for such nuclei would confirm the predictions of Danos.[6] The nuclei terbium, tantalum, and gold were chosen for study[7] because they were available in moderate quantities in monoisotopic form.

* This work supported by U. S. Atomic Energy Commission.
† On educational leave at Massachusetts Institute of Technology, Cambridge, Massachusetts.
[1] R. Nathans and J. Halpern, Phys. Rev. **93**, 437 (1954); R. Nathans and P. J. Yergin, Phys. Rev. **98**, 1296 (1955).
[2] Fuller, Petree, and Weiss, Phys. Rev. **112**, 554 (1958), preceding paper.
[3] K. Okamoto, Progr. Theoret. Phys. Japan **15**, 75 (1956); Phys. Rev. **110**, 1113 (1958).
[4] M. Danos, Bull. Am. Phys. Soc. Ser. II, **1**, 135 (1956).
[5] M. Goldhaber and E. Teller, Phys. Rev. **74**, 1048 (1948); J. H. D. Jensen and P. Jensen, Z. Naturforsch. **5a**, 343 (1950).
[6] M. Danos, Nuclear Phys. **5**, 23 (1958).
[7] Some of the preliminary results of this experiment were reported at the Stanford Conference on Nuclear Sizes and Density Distributions [G. M. Temmer, Revs. Modern Phys. **30**, 498 (1958)]. In agreement with these results B. M. Spicer (private communication) has also observed the splitting of the neutron production cross section for tantalum. These data were analyzed by smoothing the experimental activation curve. The authors want to thank Dr. Spicer for sending them his preliminary results.